Thermal Relaxation in Extrusion-Oriented Polyethylene Rods

T. STERZYNSKI,[1] P. CALO,[1] R. PIXA,[1] and D. GUEUGNAUT[2,*]

[1]Institut Charles Sadron (CRM-EAHP), 4-6 Rue Boussingault, F-67000 Strasbourg, France; [2]Gaz de France, Direction de la Recherche, Centre d'Etudes et de Recherches sur les Sciences et Techniques Appliquées, 361 Avenue du Président Wilson, F-93211 La Plaine-St-Denis, France

SYNOPSIS

To study how the properties of extruded medium-density polyethylene products are influenced by the microstructure, rodlike samples, whose morphology can be changed under appropriate processing conditions, were produced by extrusion. A special extrusion line was developed consisting of an extruder equipped with a cylindrical die, thermal separator, lubrication unit, and cooling die. A wide range of representative morphologies was achieved using various temperatures of polymer melt and of the cooling die (calibration unit). A significant structural gradient, determined by differential scanning calorimetry (DSC), was found in all extruded rods, depending on the thermal conditions. The molecular orientation through the section of the rods, resulting from the shear during the extrusion, was determined by Fourier transform infrared (FTIR) spectroscopy and by thermal relaxation, showing good agreement between both methods. © 1996 John Wiley & Sons, Inc.

INTRODUCTION

The flow of molten polymers through dies and channels during processing usually leads to preferential orientation of the macromolecular chains in the flow direction. An important velocity gradient is observed through the cross section because of the high viscosity of molten polymers. Therefore, the flow-induced orientation can be strongly heterogeneous. Beside this effect, a competition between the development of orientation (inducing a decrease of the entropy) and the development of a crystallinity gradient (due to the very low thermal conductivity) is usually noted, especially in the fast crystallizing polyethylene (PE).

Two very different zones of flow stresses occur generally in extruded full profiles (rods): shearing flow near the wall of the channel and elongational flow in the center. The velocity profile can be directly detected and measured without contact by using the laser Doppler anemometer method.[1-3] It follows from such measurements that in the center of the flow—where almost no velocity gradient exists—only elongation of the molten polymer occurs, followed by relaxation of the molecules. A significant velocity gradient is observed, on the contrary, in the near wall part of the flow, resulting in some cases in shear-induced crystallization.[4] This can lead to the development of a structure gradient as well as to the variation of molecular orientation in the cross section of the extruded profiles.

The same effects (shearing in the outer part and elongation in the center) are also observed in the cylindrical flow of molten polypropylene.[5] McHugh[6] observed that high-pressure extrusion, followed by well-controlled cooling and with important elongation, improves the mechanical properties due to the constitution of shish-kebab structures.

Characterization of the Orientation

Macromolecular orientation can be characterized by various methods. The most commonly used are direct methods based on structure measurements—by X-ray diffraction,[7] birefringence,[8] or infrared spectroscopy[9]—or indirect ones, e.g., by the evaluation of the anisotropy of thermal properties.[10,11] Another orientation parameter is, however, obtained by each of these methods; therefore, the results can only be compared qualitatively.

* To whom correspondence should be addressed.

Journal of Applied Polymer Science, Vol. 60, 1201–1208 (1996)
 CCC 0021-8995/96/081201-08

Wide-angle X-ray scattering (WAXS) allows one to observe changes of the unit cell parameters. Swan[12] measured the unit parameters of high-density polyethylene (HDPE) at different temperatures and found significant changes of the a and b parameters but no changes of the main period c. For the same polymer, Kobayashi and Keller[13,14] determined the changes of the c parameter with temperature. Similar measurements were performed also by use of synchrotron radiation.[15]

Choy et al.[16] determined the linear thermal expansion in directions parallel and perpendicular to the preferred orientation between 5 and 300 K. They proposed a layer-structure model to account for the results in which partly aligned crystalline layers embedded in an isotropic amorphous matrix are connected by stiff intercrystalline bridges. Wolf and Karl[17] published similar investigations showing a strong difference between thermal contraction for parallel measurements and expansion for perpendicular ones.

An important temperature gradient is always observed during cooling of extruded or injection-molded pieces due to the very low thermal conductivity of PE. The very high cooling rate in the skin due to direct contact with the walls of the injection mold or of the calibration unit leads to quite instantaneous solidification. The core stays, on the contrary, in the molten state for some time, depending on the thickness of the part. For this reason, solidification first induces compression in the center and elongation in the outer parts and a reversed state of residual stresses after the cooling process is finished.

Struik[18] and Kubat and Rigdahl[19] proposed a mathematical approximation of the residual stress relaxation as a function of elongation and of relaxation time. They annealed samples to eliminate the residual stresses and to decrease the state of orientation produced during polymer processing. Their modeling was performed for constant elongation and the stress relaxation was combined with the thermal-aging parameters.

Numerous authors used polarized infrared spectroscopy for the determination of orientation. The possibility to measure orientation separately for crystalline and for amorphous domains is the main advantage of this method.[20] Infrared spectroscopy as a relatively simple method is preferred for the measurement of orientation in such polymers where the corresponding crystalline and amorphous bands are easily found.[21] For PE, the authors proposed mostly the band at 1896 cm^{-1} for the crystalline domains and the band at 1305 cm^{-1} for the amorphous ones.

It is known that the mechanical properties depend on the processing conditions where, especially, the flow ratio and cooling rate are responsible for the development of the structural character. The aim of our work was to determine the state of macromolecular orientation and its distribution through the cross section of extruded PE rods as a function of varying thermal processing conditions. This article presents only the structural part of the experiments, which will be followed by the presentation of mechanical experiments performed on rods with a well-defined structure.

EXPERIMENTAL

Materials

Experiments were carried out on a commercial medium-density PE grade manufactured by Solvay & Cie, Laboratoire Central, Belgium. Its main characteristics are as follows: density 0.949 g/cm^3 at 23°C (ASTM D 1505); molecular weight $\bar{M}_w$ between 180,000 to 200,000 g/mol; polydispersity about 10, containing only about 6 butyl branches per 1000 carbons; and carbon black content of about 2.3 wt %. This resin is widely used on the gas-distribution market.[22] A similar carbon black-free resin (Eltex B 6920) was also used for comparison.

Extrusion and Calibration of the Rods

Rods with a diameter of 8 mm were extruded using an extrusion line composed of a FAIREX extruder with a screw diameter of 30 mm and a length to diameter ratio L/D = 24. It was equipped with a cylindrical die with a diameter of 8 mm and a ratio L/D of 4.5. The die was provided with a converging inlet to reduce the flow diameter from 30 mm (screw output) to 8 mm. The final rod diameter was obtained with a slightly divergent die cross section. The increase of the output diameter should limit the effect of the extrudate swell leading normally to irregularities in the extrudate shape.

The extrusion die and the calibration unit (cooling die) were connected.[23,24] A thermal separation and a lubrication unit were inserted between the extrusion die and the calibration unit. The role of the thermal separation was to reduce effectively the axial heat flow from the hot extrusion die to the tempered calibration unit. The lubricating unit was intended to facilitate slippage of the extruded rod

on the wall of the calibration unit. Low-viscosity silicon oil was used as a lubricant. Its quantity and pressure were adjusted to assure both a constant lubricating film and to keep permanent contact between the extruded polymer and the wall of the calibration unit.

The rods were cooled in a calibration unit with the temperature control in the range from 15 to 90°C. To avoid the formation of voids in the extruded rods (resulting both from the very fast crystallization of the skin layer and important crystallization shrinkage), the extrusion was accomplished with a very low mass flow ratio, giving a mean extrusion speed of about 12.5 cm/min. As the length of the conformation unit was 30 cm (with a well-defined wall temperature T_c), the mean cooling time was of the order of 2.4 min. Such a low extrusion rate under a relatively high extrusion pressure allowed us to achieve a high packing pressure in the molten polymer and during crystallization, giving PE rods free of shrinkage cavities which are usually observed in the center of PE products with high wall thickness.

Extrusions were performed with different processing parameters, by varying both the temperatures of the extrusion die (T_m between 180 and 245°C) and of the calibration unit (T_c = 16, 30, 50, and 70°C). The nomenclature that we use subsequently for the samples is of the type T_m/T_c.

Crystallinity

Differential scanning calorimetry (DSC) measurements were performed on several points on the section of the rods to characterize the radial crystallinity gradient. Due to its easier utilization, the DSC technique was preferred to the somewhat more accurate density measurement method, both techniques being well correlated.[25] Samples for the DSC investigations with a thickness of 200 microns were cut using a Leitz 1300 microtome. The measurements were done using a Perkin-Elmer DSC 4 apparatus under constant heating rate of 10 K/min. The melting enthalpy ΔH_m was measured from the area of the melting peaks between 30 and 141.5°C by taking a value of 8.22 kJ/mol for pure crystalline PE,[26] which corresponds to 293 J/g. Figure 1 presents an example of a typical DSC thermogram. The crystallinity of the samples was always measured during the first heating scan, so the results represent their real crystallinity corresponding to the thermomechanical history produced by the extrusion process.

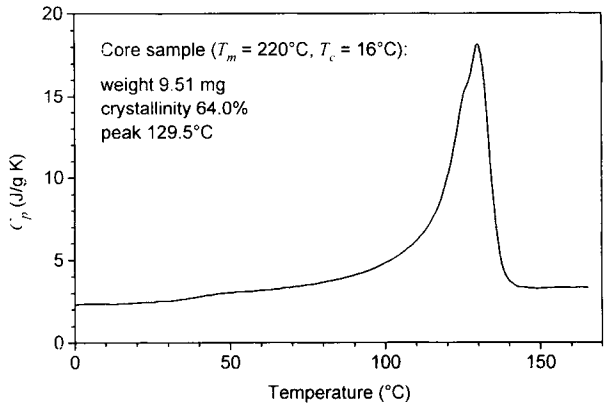

Figure 1 Typical DSC thermogram of carbon black-containing sample extruded at T_m = 220°C and calibrated at T_c = 16°C.

Preliminary experiments were carried out on one representative sample with six consecutive heating–cooling cycles between 0 and 150°C to test the reproducibility of the crystallinity measurements by this method. The average crystallinity of this sample amounts to 63.84% with an estimated standard deviation of 0.10%.

Fourier Transform Infrared Spectroscopy

FTIR measurements were used for the determination of molecular orientation of the extruded rods. The apparatus used was a Nicolet 60SX spectrometer equipped with polarizing filters.

The orientation of extruded PE was determined using two absorption bands: a crystalline one (CH_2 rocking at 1896 cm^{-1}) and an amorphous one (CH_2 twisting + CH_2 asymmetric wagging at 1305 cm^{-1}).[25] The dichroic ratio D, Hermans orientation function f, and the average value of the angle ϕ between the flow direction and the polymer chains were evaluated from the infrared measurements.

The dichroic ratio D for each band is calculated from

$$D = \frac{A_{\parallel}}{A_{\perp}} \tag{1}$$

where $A_{\parallel}$ and $A_{\perp}$ are the optical densities with polarizer, respectively, parallel and perpendicular to the main flow axis. In the transmission mode, the optical density for a given wavelength is evaluated as

$$A = \log \frac{I_0}{I} = d\alpha c_a \tag{2}$$

where I_0 represents the incident light intensity; I, the transmitted light intensity at maximum absorbance; d, the sample thickness; α, the absorption coefficient; and c_a, the absorbant group concentration.

The Hermans orientation function is defined as

$$f = \frac{3\langle\cos^2\phi\rangle - 1}{2} \tag{3}$$

The relationship between the orientation function f for the c-axis and the dichroic ratio for a particular band is given as[27]

$$f = \frac{(D-1)(D_0+2)}{(D+2)(D_0-1)} \tag{4}$$

where θ represents the angle between the c-axis and the dipole moment, D is the measured dichroic ratio, and $D_0 = 2\cot^2\theta$.

The dipole moment for the crystalline band at 1896 cm^{-1} is almost perpendicular to the c-axis (i.e., $\theta = 90°$) according to Krimm.[28] Therefore, $D_0 = 0$ and

$$f = -2\frac{D-1}{D+2} \tag{5}$$

For the amorphous band at 1305 cm^{-1}, it can also be taken into account that the dipole moment is nearly parallel to the c-axis ($\theta = 0°$), i.e., $D_0 = \infty$ and

$$f = \frac{D-1}{D+2} \tag{6}$$

Thermal Expansion During Annealing

The macromolecular orientation was measured indirectly by recording linear expansion during annealing. The samples were heated in an oil bath maintained at constant temperature (100°C). Each sample was submitted to the same thermal treatment, combining two cycles of alternating heating and cooling.

The deformation of the samples was measured with an inductive linear transducer and recorded on an X–Y recorder. The experimental setup allowed measurement resolution of thermally induced linear deformation better than 4 μm.

RESULTS

Crystallinity Distribution

The crystallinity x_c was determined from DSC melting thermograms at several points through the radius of the extruded rods. The DSC scans were performed from 20 to 170°C, with the maximum of the melting curve taken as the melting temperature. For the samples taken on the various positions through the section of the extruded rods, we did not observe any important changes of the melting temperature or of the crystallization temperature. The mean melting temperature was about 129°C for all samples.

It is known that in the case of low-density PE the slow changes of the DSC melting curves make the determination of the temperature of the beginning of the melting process rather difficult. This was clearly not the case in the investigated samples (cf. Fig. 1).

Figure 2 presents the radial distribution of x_c for the rods extruded from both resins, with and without carbon black. Lower x_c values are observed in the outer part compared to the center of the rods for both melt temperatures, T_m (180 and 245°C), as well as for both calibration unit temperatures, T_c (70 and 16°C).

A lower crystallinity is observed on the carbon black containing samples extruded at 245°C and calibrated at 16°C, when compared to the carbon black-free samples. It amounts to about 5% in the core but only to 2% in the skin. This lowering is either due to the presence of some nucleating additives in the carbon black-free samples or to an inhibiting effect of the carbon black. In the 180/70 samples, a decrease of crystallinity is still observed in the core, however, at a lower level.

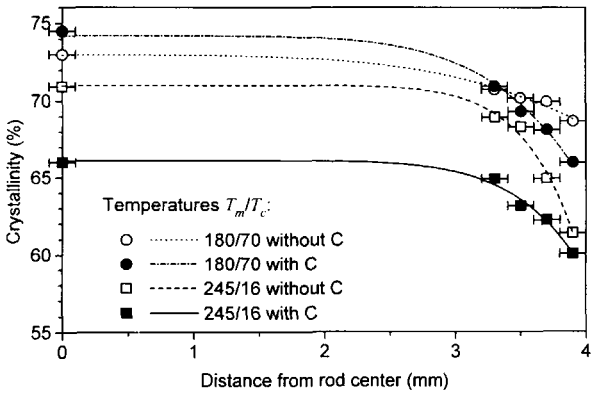

Figure 2 Influence of carbon black on the radial crystallinity distribution of samples extruded at melt temperatures T_m = 180°C (respectively, 245°C) and calibration unit temperatures T_c = 16°C (respectively, 70°C).

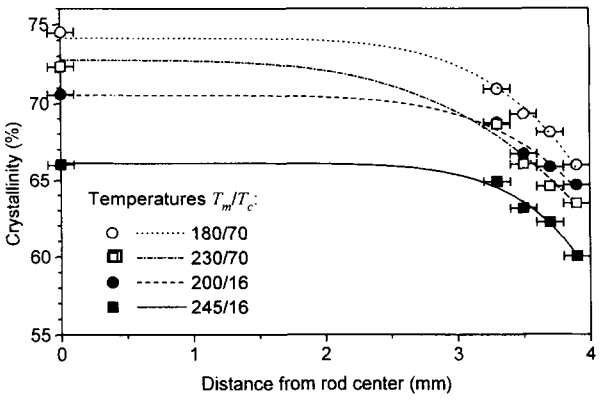

Figure 3 Influence of melt temperatures T_m (180, 200, 230, 245°C) and calibration unit temperatures T_c (16, 70°C) on the radial crystallinity distribution in extruded samples.

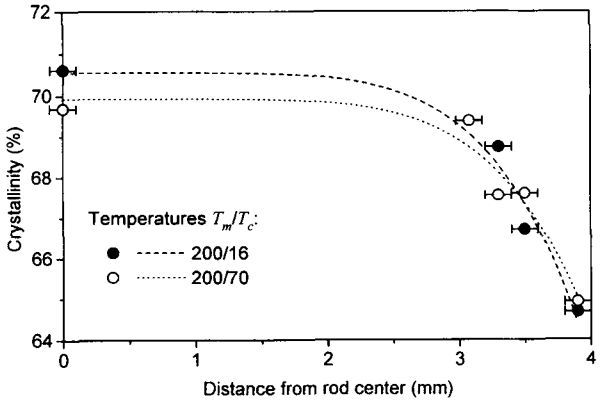

Figure 4 Influence of calibration unit temperature T_c (16, 70°C) on radial crystallinity distribution in samples extruded at T_m = 200°C.

Figures 3 and 4 present the influence of temperature conditions on the radial crystallinity distributions of carbon black-filled samples. Figure 3 shows crystallinity profiles for the calibration unit temperatures, T_c = 16 and 70°C, both for two different melt temperatures. A higher crystallinity for lower-temperature differences, $\Delta T = T_m - T_c$, is observed for all conditions. This tendency is also visible by comparing samples with the constant melt temperature (T_m = 200°C) and variable calibration unit temperatures T_c of 70 and 16°C, respectively (Fig. 4). In this case, the differences ΔT are much smaller (130 and 184°C, respectively) and the crystallinity differences appear not significant. An important radial structure gradient, i.e., a lowering of x_c in the outer part of the rods, is observed in all cases.

The much higher cooling rate in the outer part of the rods is probably at the origin of these observations. A very fast cooling in the outer layer which was in direct contact with the calibration unit can even lead to the formation of a thin amorphous skin followed by a radial structure gradient. This was observed for other semicrystalline polymers, as, e.g., polypropylene. Although more complex, similar trends were obtained on 110 mm-thick PE gas pipes extruded from the same resin.[29]

Thermally Induced Deformation

The state of macromolecular orientation was determined using thermal deformation measurements. The measurements were done separately for the skin and for the core of the extruded rods. Full cylindrical samples of the center part with a diameter of 4 mm and hollow cylindrical ones of the outer part with a thickness of 2 mm were prepared. The machining was made under appropriate conditions to maintain the state of orientation produced by extrusion.

During heating and cooling of partly oriented samples, different effects can occur:

- Reversible thermal expansion of both the amorphous (Δl_a) and the crystalline domains (Δl_c).
- Anisotropic deformation of amorphous domains due to orientation relaxation (Δl_r).
- Recrystallisation (secondary crystallization) and stress relaxation, both which we consider to be insignificant for the thermally induced dimensional changes.

The aspect of linear thermal deformation of partly oriented samples of a semicrystalline polymer during two heating–cooling cycles is schematically presented on Figure 5. During the first heating, both thermal expansion and orientation relaxation occur, leading to a measured total expansion Δl_1:

$$\Delta l_1 = \Delta l_a + \Delta l_c + \Delta l_r \qquad (7)$$

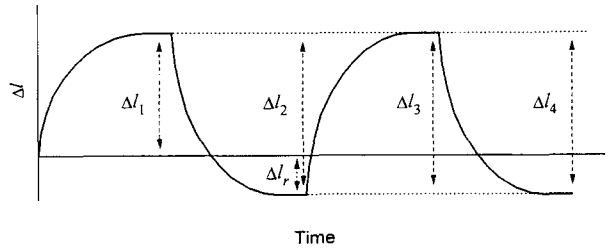

Figure 5 Linear thermal deformations of an oriented semicrystalline sample during two consecutive heating–cooling cycles.

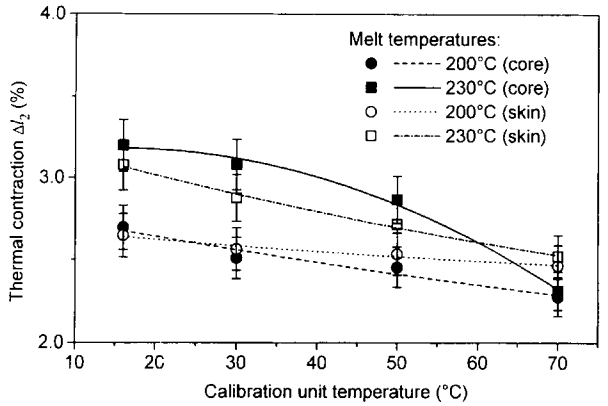

Figure 6 Linear thermal deformation Δl_r due to orientation release of central and outer parts of samples extruded at two melt temperatures T_m (200, 230°C) vs. calibration unit temperature T_c.

During the following first cooling, the measured shrinking of the previously annealed polymer is exclusively due to thermal contraction:

$$\Delta l_2 = -(\Delta l_a + \Delta l_c) \tag{8}$$

During the second heating, only thermal expansion occurs ($\Delta l_3 = -\Delta l_2$). The ultimate cooling shows exclusively the corresponding thermal contraction: $\Delta l_4 = \Delta l_2$.

The importance of thermal contraction Δl_2 depends on the crystallinity of the sample, as amorphous and crystalline phases have very different thermal expansivities. From the literature data,[30] a linear coefficient of thermal expansion β_c of $(1 \pm 0.2) \cdot 10^{-4}$ K^{-1} for pure crystalline PE and a coefficient β_a of $(2.4 \pm 0.3) \cdot 10^{-4}$ K^{-1} for pure amorphous PE are deduced. Consequently, Δl_2 must be lower in samples of higher crystallinity.

The variation of the linear thermal contraction Δl_2 vs. the calibration unit temperature is presented in Figure 6 for the core and for the outer part of the rods. We see that the absolute value of Δl_2 decreases with increasing calibration unit temperature. As mentioned, the lower thermal expansion should be due to higher crystallinity, which can primarily be explained by the smaller differences ΔT between the polymer melt temperature and the calibration unit temperature.

The orientation release Δl_r is supposed to belong only to the amorphous phase. By using the experimental values Δl_1 and Δl_2 and knowing the crystallinity of the sample, we define a normalized coefficient C to quantify the state of orientation of the amorphous phase:

$$C = \frac{\Delta l_r}{1 - x_c} = \frac{\Delta l_1 + \Delta l_2}{1 - x_c} \tag{9}$$

Negative values of the C coefficient are representative for the case where an orientation in the flow direction took place during extrusion. On the contrary, a positive C coefficient indicates that the expansion on heating (Δl_1) was greater than the contraction on cooling (Δl_2). In this case, the preferential direction of the macromolecular chains was perpendicular to the flow direction.

Figure 7 presents the variation of the C coefficient as a function of the calibration unit temperature for two melt temperatures: 200 and 230°C, both for the core of the rod (C_c) and for the outer surface (C_s). The coefficient C_s is negative in most cases, i.e., the amorphous segments of the molecules in the skin of extruded samples were predominantly oriented in the flow direction. Values of C_s near zero correspond to the situation where no orientation existed, which is observed only for the low T_c for the outer part of the rods.

The positive C_c values can be explained by the following simplified model[18]: During the cooling in the calibration unit, rapid solidification of rod skin took place. The created rigid shell contracted, which was counteracted by the still fluid core. But due to its small stiffness, hardly any stresses were built up, neither in the skin nor in the core. The latter crystallized subsequently progressively inward. The contraction produced by the densification then induced orientation of the amorphous segments in the radial direction.

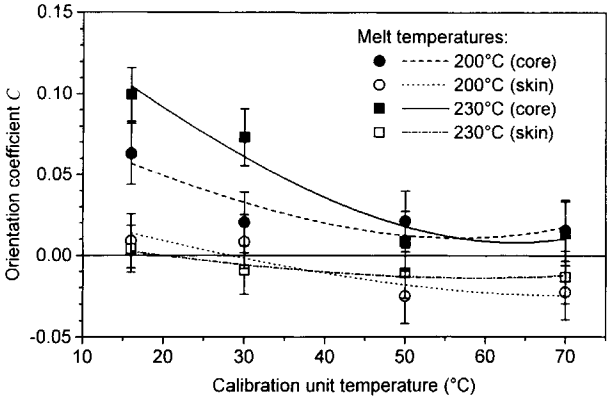

Figure 7 Variation of the orientation coefficient C of central and outer parts of samples extruded at two melt temperatures T_m (200, 230°C) vs. calibration unit temperature T_c.

Orientation Determined by Infrared Spectroscopy

The value of the Hermans orientation function for the crystalline domains is always higher for the lower melt temperature. It reaches values between 0.07 and 0.15 for a melt temperature of 200°C and values between 0.05 and 0.11 for 230°C. The orientation coefficient for the amorphous domains is rather small and remains constant vs. the calibration unit temperature, i.e., when the difference between the melt temperature and the calibration unit temperature decreases.

The term

$$\langle\phi\rangle = \arccos\sqrt{\frac{2f+1}{3}} \qquad (10)$$

characterizes the average value of the angle between the flow direction and the crystallographic c-axis. It follows from the definition of the Hermans orientation function that the angle $\langle\phi\rangle = 54.74°$ denotes the isotropic state, which corresponds to $f = 0$. An angle $\langle\phi\rangle$ lower than 54.74° indicates orientation in the flow direction. Figure 8 presents the mean values of the angle $\langle\phi\rangle$ vs. the calibration unit temperature for the amorphous and crystalline domains.

For the amorphous domains, the values are rather small and quite independent of the calibration unit temperature. For the crystalline domains, a certain decrease of the $\langle\phi\rangle$ angle (i.e., higher orientation) with decreasing ΔT (i.e., with increasing viscosity of the molten polymer) is observed. It is known that usually much higher crystallization rates are observed at lower temperatures. Therefore, the higher state of orientation can be the effect of the less effective relaxation process due both to the higher crystallization rate at lower melt temperature and to the shorter cooling time.

CONCLUSION

We observed significant structural changes, although the only variable processing parameters were melt temperature and calibration unit temperature. We noted crystallinity gradients in all cases, with higher values in the core of the extruded rods and lower ones in the skin. Higher average crystallinity was, however, produced by lower temperature differences between melt and calibration temperatures. We established the following points concerning molecular orientation:

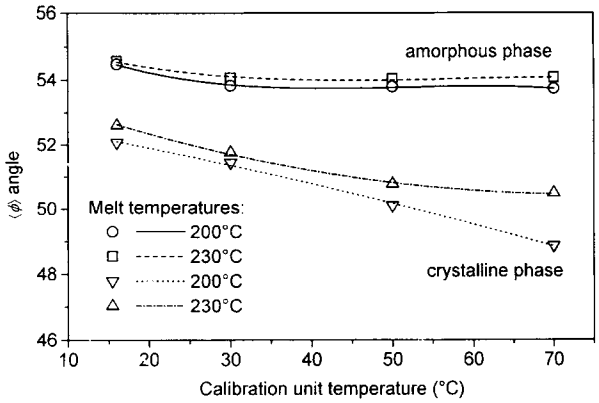

Figure 8 Mean angles $\langle\phi\rangle$ of amorphous and crystalline phases vs. calibration unit temperature.

- The amorphous phase in the rod skin is much less oriented compared to the crystalline domains.
- The average orientation increases when the melt temperature decreases and the calibration unit temperature increases (increase of the viscosity of the polymer).
- The influence of the calibration unit temperature is more significant than that of the polymer melt.

Hence, for the production and use of extruded products with important wall thickness (e.g., rods, gas, and water pipes), it is important to consider that the thermal processing conditions are responsible not only for the formation of the structure but also for the dimensional stability through the development of molecular orientation.[31]

NOMENCLATURE

a	crystallographic unit cell parameter
$A_{\parallel}$	optical density with polarizer parallel to the main flow axis
$A_{\perp}$	optical density with polarizer perpendicular to the main flow axis
b	crystallographic unit cell parameter
c	crystallographic unit cell parameter
c_a	absorbant group concentration
C	coefficient proportional to the orientation, calculated from thermal expansion
C_c	orientation coefficient in the core of the rod
C_s	orientation coefficient in the skin of the rod
d	sample thickness
D	dichroic ratio
D_0	$2\cot^2\theta$

f	Hermans orientation function
ΔH_m	melting enthalpy
I	intensity of transmitted light at maximum absorbance
I_0	intensity of incident light
Δl_a	thermal expansion of the amorphous phase
Δl_c	thermal expansion of the crystalline phase
Δl_i	thermal expansion during the ith heating cycle (i = 1, 2, 3, 4)
Δl_r	deformation produced by relaxation of molecular orientation in the amorphous phase
$\bar{M}_w$	weight-average molecular weight
ΔT	temperature difference between T_m and T_c
T_c	temperature of the calibration unit
T_m	temperature of the extrusion die (=melt temperature)
x_c	crystallinity

Greek Letters

α	absorption coefficient
β_a, β_c	linear coefficients of thermal expansion of amorphous, viz., crystalline PE
ϕ	angle between flow direction and the c-axis
$\langle\phi\rangle$	average value of the angle between flow direction and the c-axis
θ	angle between c-axis and the dipole moment

REFERENCES

1. H. Kramer and J. Meissner, in *Rheology 2, Fluids,* G. Astarita, Ed., Plenum Press, New York, 1980.
2. J. Meissner, *Polym. Test.*, **3,** 291 (1983).
3. T. Sterzynski, *J. Mater. Sci.-Phys. B,* **27,** 369 (1988).
4. H. Janeschitz-Kriegl and F. Kügler, in *Polymer Processing and Properties,* G. Astarita, Ed., Plenum Press, New York, 1985.
5. T. Ariyama, *Polym. Eng. Sci.*, **31,** 1101 (1991).
6. A. J. McHugh, *Int. Polym. Process.*, **4,** 208 (1991).
7. L. E. Alexander, *X-ray Diffraction Methods in Polymer Science,* Wiley-Interscience, New York, 1969.
8. D. A. Hensley, *The Light Microscopy of Synthetic Polymers,* Oxford University Press, Oxford, 1984.
9. I. M. Ward, *Adv. Polym. Sci.*, **66,** 81 (1985).
10. K.-H. Hellwege, J. Hennig, and W. Knappe, *Kolloid-Z. Z. Polym.*, **188,** 121 (1963).
11. T. Sterzynski and J. J. Linster, *Polym. Eng. Sci.*, **27,** 906 (1987).
12. P. R. Swan, *J. Polym. Sci.*, **56,** 403 (1962).
13. M. Kobayashi, *J. Chem. Phys.*, **70,** 509 (1979).
14. M. Kobayashi and A. Keller, *Polymer,* **11,** 114 (1970).
15. T. Sterzynski, *Polimery,* **33,** 10 (1988).
16. C. L. Choy, F. C. Chen, and F. L. Ong, *Polymer,* **20,** 1191 (1979).
17. F. P. Wolf and V. H. Karl, *Coll. Polym. Sci.*, **259,** 29 (1981).
18. L. C. E. Struik, *Polym. Eng. Sci.*, **18,** 799 (1978).
19. J. Kubat and M. Rigdahl, *Int. J. Polym. Mater.*, **3,** 287 (1981).
20. R. Zbinden, *Infrared Spectroscopy of High Polymers,* Academic Press, New York, 1964.
21. R. Stein and F. Norris, *J. Polym. Sci.*, **21,** 381 (1956).
22. D. Gueugnaut, G. Lappai, P. Vautherin, and D. Reveret, in *Proceedings of the 12th Annual International Conference on Advances in Stabilization and Controlled Degradation of Polymers,* Lucerne, Switzerland, May 1990, p. 95.
23. W. Michaeli, *Extrusion Dies for Plastics and Rubber,* 2nd ed., Hanser, Munich, 1992.
24. T. Sterzynski, C. Gandon, K. Boytard, and D. Gueugnaut, in *Proceedings of the Bayreuth Polymer and Materials Symposium,* Bayreuth, Germany, April 1993, p. 193.
25. D. Gueugnaut, P. Wackernie, and J. P. Forgerit, *J. Appl. Polym. Sci.*, **35,** 1683 (1988).
26. D. W. van Krevelen, *Properties of Polymers,* 3rd ed., Elsevier, Amsterdam, 1990, p. 120.
27. B. E. Read and R. S. Stein, *Macromolecules,* **1,** 116 (1968).
28. S. Krimm, *Fortschr. Hochpolym. Forsch.*, **2,** 95 (1960).
29. D. Gueugnaut, P. Relet, and D. Rousselot, in *Proceedings of the 1992 International Gas Research Conference,* Orlando, FL, November 1992, p. 889.
30. D. W. van Krevelen, *Properties of Polymers,* 3rd ed., Elsevier, Amsterdam, 1990, p. 92.
31. D. Gueugnaut, K. Boytard, L. Paviet, R. Pixa, and T. Sterzynski, in *Proceedings of the Polymer Processing Society,* Strasbourg, France, August 1994, p. 81.

Received February 3, 1995
Accepted November 30, 1995